Parametric study of hydrogen production via sorption enhanced steam methane reforming in a circulating fluidized bed riser

Kiattikhoon Phuakpunk [a], Benjapon Chalermsinsuwan [b,c,d,*], Sompong Putivisutisak [d,e], Suttichai Assabumrungrat [a,d]

[a] Center of Excellence in Catalysis and Catalytic Reaction Engineering, Department of Chemical Engineering, Faculty of Engineering, Chulalongkorn University, Bangkok 10330, Thailand
[b] Fuels Research Center, Department of Chemical Technology, Faculty of Science, Chulalongkorn University, Bangkok 10330, Thailand
[c] Center of Excellence on Petrochemical and Materials Technology, Chulalongkorn University, Bangkok 10330, Thailand
[d] Advanced Computational Fluid Dynamics Research Unit, Chulalongkorn University, Bangkok 10330, Thailand
[e] Department of Mechanical Engineering, Faculty of Engineering, Chulalongkorn University, Bangkok 10330, Thailand

HIGHLIGHTS

- Kinetics of steam methane reforming and carbonation were incorporated in CFD model.
- 2^k factorial design was used to analyze parameters.
- Hydrogen purity could reach equilibrium as well as that conducted in bubbling bed.
- Gas velocity, riser diameter and solid flux had major effects on system designing.
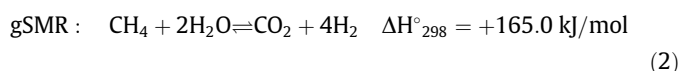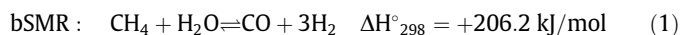
ARTICLE INFO

ABSTRACT

Computational fluid dynamics was applied for sorption enhanced steam methane reforming (SESMR) operating in a circulating fluidized bed (CFB) riser. The solid mixtures consisted of Ni-based catalyst and CaO sorbent. The aim of study was to design a proper pilot-scale CFB riser which produced hydrogen (H_2) with both high purity and high flux. The design parameters and the reaction parameters were examined with 2^k full factorial design. The significances of each parameter were analyzed by analysis of variance. Using the optimum result, the highest H_2 purity reached 98.58% in dry basis accompanied with the highest H_2 flux of 0.301 kg/m^2 s. The hydrodynamics of this optimum case showed that SESMR was nearly completed since 5.0 m height because axial and radial distributions of solid were well developed without excessive segregation between catalyst and sorbent. Thus, the H_2 purity and the H_2 flux approached fully developed within the riser height.

© 2018 Elsevier Ltd. All rights reserved.

1. Introduction

Conventional industrial-level hydrogen production has used methane (CH_4), in natural gas or in tail gas from refinery process, as raw material via steam methane reforming (SMR) process. The conventional processes consist of three main sections i.e. reforming, shifting and gas separation (Harrison, 2008). In reforming and shifting section, maximum CH_4 is converted to mainly CO_2 and H_2 (with little of CO) via three reversible reactions including steam methane reforming (bSMR and gSMR) reactions and water-gas shift (WGS) reaction as shown below.

$$bSMR: \quad CH_4 + H_2O \rightleftharpoons CO + 3H_2 \quad \Delta H^\circ_{298} = +206.2 \text{ kJ/mol} \quad (1)$$

$$gSMR: \quad CH_4 + 2H_2O \rightleftharpoons CO_2 + 4H_2 \quad \Delta H^\circ_{298} = +165.0 \text{ kJ/mol} \quad (2)$$

$$WGS: \quad CO + H_2O \rightleftharpoons CO_2 + H_2 \quad \Delta H^\circ_{298} = -41.2 \text{ kJ/mol} \quad (3)$$

By thermodynamic equilibrium, a high temperature above 750 °C is sufficient to maximize conversion of CH_4 in a reforming furnace. The effluent gas of the furnace which still containing CO about 8–10% in dry basis is then fed to WGS reactors including high temperature shift (HTS) reactor, operating at 300–400 °C, and low temperature shift (LTS) reactor, operating at 200–300 °C, in series. The outlet gas from the second shift reactor approximately consists of 76% H_2, 17% CO_2, 4% unreformed CH_4 and 3% CO in dry basis

* Corresponding author at: Fuels Research Center, Department of Chemical Technology, Faculty of Science, Chulalongkorn University, Bangkok 10330, Thailand.
E-mail address: Benjapon.C@chula.ac.th (B. Chalermsinsuwan).

Nomenclature

C_D	Drag coefficient, [–]
$C_{fr,ls}$	Friction coefficient between solid phases, [–]
Cat/Sb	Catalyst to sorbent ratio, [kg·kg^{-1}]
d_s	Particle diameter of solid phase, [m]
$e_{ss} \equiv e_{ls}$	Restitution coefficient for solid-solid collisions, [–]
f_{drag}	Drag function
G_s	Solid flux, [kg·m^{-2}·s^{-1}]
$\vec{g}$	Gravity force, [m·s^{-2}]
$g_{0,ls}$	Radial distribution coefficient of mutual solid phases, [–]
$g_{0,ss}$	Radial distribution coefficient of single solid phase, [–]
H	Height of the riser, [m]
H_g	Specific enthalpy of gas phase, [m^2·s^{-2}, J·kg^{-1}]
H_j	Specific enthalpy of species j in the reaction, [m^2·s^{-2}, J·kg^{-1}]
H_j^f	Specific heat of formation of species j in the reaction, [m^2·s^{-2}, J·kg^{-1}]
$h_{sg} \equiv h_{gs}$	Gas-solid interphase heat exchange coefficient, [m^2·s^{-2}, J·kg^{-1}]
$\bar{I}$	Unit tensor, [–]
id	Diameter of the riser, [m]
$\vec{J}_k^q$	Mass flux of species k into phase q, [kg·m^{-2}·s^{-1}]
K_i	Equilibrium constants of reaction i
K_k	Adsorption equilibrium constants of species k
$K_{ls} \equiv K_{sl}$	Solid-solid interphase momentum exchange coefficient, [kg·m^{-3}·s^{-1}]
$K_{sg} \equiv K_{gs}$	Gas-solid interphase momentum exchange coefficient, [kg·m^{-3}·s^{-1}]
k_{carb}	Rate constants of carbonation
k_g	Thermal conductivity of gas phase, [W·m^{-1}·K^{-1}]
k_i	Rate constants of reaction i
k_{Θ_s}	Diffusion coefficient, [m^2·s^{-1}]
M_j	Molecular weight of species j in the reaction, [kg·kmol^{-1}]
$\dot{m}_{pq}$	Mass transfer from phase p to phase q, [kg·m^{-3}·s^{-1}]
Nu_s	Nusselt number of solid phase, [–]
n	Degree of partial pressure, [–]
Pr	Prandtl number of gas phase, [–]
p	Static pressure, [Pa]
p_{CO_2}	Partial pressure of CO$_2$, [Pa]
$p_{CO_2,eq}$	Equilibrium pressures of CO$_2$, [Pa]
p_g	Static pressure of gas phase, [Pa]

p_k	Partial pressures of species k, [Pa]
p_s	Solid pressure, [Pa]
Q_{sg}	Intensity of heat exchange between solid phase and gas phase, [W·m^{-3}]
$\vec{q}_g$	Heat flux of gas phase, [W·m^{-2}]
R	Rate of a heterogeneous reaction, [kmol·m^{-3}·s^{-1}]
R_k^q	Net rate of species k produced by homogeneous reactions inside phase q, [kg·m^{-3}·s^{-1}]
Re_s	Particle Reynolds number of solid phase, [–]
r_{carb}	Rate of carbonation, [kmol·kg$_{sorb}^{-1}$·s^{-1}]
r_i	Rates of reaction i, [kmol·kg$_{cat}^{-1}$·s^{-1}]
$S_{h,g}$	Heat source of gas phase, [W·m^{-3}]
S_k^q	Rate of creation of species k by addition from dispersed phase and other sources in phase q, [kg·m^{-3}·s^{-1}]
$S_{m,q}$	Mass source of phase q, [kg·m^{-3}·s^{-1}]
S_0	Initial specific surface area of CaO, [m^2·kg$_{sorb}^{-1}$]
S/C	Steam to carbon, [mol·mol^{-1}]
T_{in}	Temperature of inlets, [°C]
U	Gas inlet velocity, [m·s^{-1}]
$\vec{v}_{ls}$	Interphase velocity from phase l (solid or gas) to solid phase, [m·s^{-1}]
$\vec{v}_q$	Velocity of phase q, [m·s^{-1}]
$\vec{v}_{r_j}$	Velocity of a reactant j which involved in the reaction, [m·s^{-1}]
$\vec{v}_{sg}$	Interphase velocity from solid phase to gas phase, [m·s^{-1}]
X_{CaO}	Conversion of CaO, [–]
Y_k^q	Mass fraction of species k in phase q, [–]
γ_j	Stoichiometric coefficient of species j in the reaction, [–]
ε_q	Volume fraction of phase q, [–]
$\varepsilon_{s,max}$	Maximum packing of solid phase, [–]
Θ_s	Granular temperature, [m^2·s^{-2}, J·kg^{-1}]
λ_q	Bulk viscosity of phase q, [Pa·s]
λ_s	Solid bulk viscosity, [Pa·s]
μ_q	Shear viscosity of phase q, [Pa·s]
μ_s	Solid shear viscosity, [Pa·s]
$\mu_{s,col}$	Collisional viscosity of solid phase, [Pa·s]
$\mu_{s,fr}$	Friction viscosity of solid phase, [Pa·s]
$\mu_{s,kin}$	Kinetic viscosity of solid phase, [Pa·s]
ρ_q	Physical density of phase q, [kg·m^{-3}]
$\bar{\tau}_q$	Stress tensor of phase q, [Pa]
τ_s	Particulate relaxation time in solid phase, [s]

(Harrison, 2008). Thereafter, H$_2$ is separated through separation units such as pressure swing adsorption (PSA) or amine scrubbing technology (Barelli et al., 2008). These conventional processes use many units, utilities and resources.

A new concept of sorption enhanced steam methane reforming (SESMR) has been raised because of the advantages taken from that CO$_2$ that adsorbed by sorbents in the same reforming reactor. For the first advantage, equilibrium of reforming reactions (1) and (2) is shifted forwardly, so H$_2$ is more produced and CH$_4$ can be almost completely converted. Another advantage is that effluent gas from the reformer has higher H$_2$ purity reaching of 99% in dry basis (Harrison, 2008; Barelli et al., 2008; Koumpouras et al., 2007; Cotton et al., 2013), thus separation units are unnecessary in the processes. However, limitation of SESMR is the discontinuous performance when the sorbent is almost full of CO$_2$ captured. The sorbent has to release CO$_2$ before reprocessing SESMR.

There are many sorbents suitable for CO$_2$ capture divided into natural sorbents such as limestone, dolomite, huntite and hydrotalcite, and synthetic sorbents such as Li$_4$SiO$_4$, Li$_2$ZrO$_3$ and Na$_2$ZrO$_3$

(Harrison, 2008; Barelli et al., 2008). Among all listed sorbents, CaO sorbents, i.e. limestone and dolomite, are the cheapest and have the highest CO$_2$ capacity, moderate adsorption rate but the lowest stability (Harrison, 2008; Barelli et al., 2008). Hydrotalcite-like materials (HTCls) have the highest adsorption rate, good stability but very low CO$_2$ capacity (Harrison, 2008; Barelli et al., 2008; Koumpouras et al., 2007). The synthetic sorbents have high capacity, good stability and low to moderate adsorption rate but are the most expensive (Ochoa-Fernandez et al., 2005; Harrison, 2008; Barelli et al., 2008; Koumpouras et al., 2007). Thus, for large-scale hydrogen production via SESMR, natural CaO sorbents such as dolomite and limestone are preferable due to their profitable costs. Even though limestone has more CO$_2$ capacity than dolomite due to higher CaO content, but dolomite contains more MgO that makes dolomite more stable to cyclic usage (Harrison, 2008; Comas et al., 2004; Aceves Olivas et al., 2014). Thus, dolomite is a suitable sorbent for large-scale processes of SESR which has to involve regeneration of the used sorbent.